

Modelling the angular momentum evolution of low-mass stars with core-envelope decoupling

S. Allain

Laboratoire d'Astrophysique, Observatoire de Grenoble, URA CNRS 708, B.P. 53, F-38041 Grenoble Cedex 9, France
(Stephanie.Allain@obs.ujf-grenoble.fr)

Received 5 June 1997 / Accepted 22 January 1998

Abstract. We present a model of angular momentum evolution for stars in the mass range $0.5 - 1.1 M_{\odot}$, during their early stages of evolution. The model is based upon the following hypothesis: a constant surface rotational period during star-disk interaction, angular momentum loss through magnetic wind, and differential rotation parameterized with a constant coupling time. We investigate the effect of the different parameters, the initial velocity at the T Tauri age, the disk lifetime, the magnetic braking law, and we discuss the effect of introducing a core-envelope decoupling. The angular momentum transfer is parameterized by the use of a coupling time scale τ_c , which controls the exchanges of angular momentum between the – fast-rotating – radiative core and the convective envelope, both supposed to rotate as solid bodies. We present evolutionary tracks of a single star through the pre-main sequence and the main-sequence, for different masses and different coupling time-scales. We conclude that rapid rotators require solid-body rotation, and ZAMS slow rotator require a strong differential decoupling with a characteristic coupling time about 100 Myr.

Key words: stars: rotation – stars: late-type – stars: pre-main sequence – stars: interiors

1. Introduction

The different processes which drive the angular momentum evolution of young low-mass stars are contraction, internal evolution (formation and increase of the radiative core, retreat of the convective zone), interaction with surrounding environment (accretion disk, Bouvier et al. 1993), and angular momentum loss through magnetic winds (Schatzman, 1962).

The stellar contraction and the apparition of the radiative core in the inner parts are at the origin of a density gradient inside the star and hence, local conservation of angular momentum leads to a large velocity gradient with radius. Convective motions enforce a rigid rotation in the envelope and a solar-type wind applies a magnetic braking to the envelope. At ZAMS ages the core then rotates far faster than the envelope. On the other hand, helioseismology tells us that the Sun rotates as a solid-

body down to at least $r = 0.2 R_{\odot}$ (Gough, 1991). Tomczyk et al. (1996) also suggests that the radiative core rotates as a solid-body. To conciliate differential rotation at ZAMS ages inferred from contraction, and quasi-solid rotation at the age of the Sun, it is necessary to suppose redistribution of angular momentum in stellar interiors.

Several processes of angular momentum transport have been proposed to reproduce the surprising rotational profile of the Sun (see Zahn 1996 for a review, and references below). Endal and Sofia (1978) treated angular momentum transfer induced by various instabilities. They introduce two different kind of instabilities: dynamical instabilities whose characteristic time scales are shorter than the evolutionary time scale of the star: convection, dynamical shear and Soldberg-Hoiland instability; and secular instabilities, whose mixing time-scales are comparable to evolutionary time-scales: Eddington circulation (1925), secular shear and Goldreich-Schubert-Fricke instability (Fricke 1968, Goldreich and Schubert 1967). They suppose that convection induces solid-body rotation in the envelope, and that angular momentum transfer in the radiative core can be treated as a pure diffusive process. Pinsonneault et al. (1989) used the same equations of diffusion than Endal & Sofia in a model of angular momentum evolution. They find that the rotational profile is mainly dependent of angular momentum transport in the radiative parts. They manage to reproduce the flat rotational profile down to a radius of $0.4 - 0.5 R_{\odot}$, and find that a very efficient diffusive process is necessary to reproduce the low velocities of the inner parts.

More recently Chaboyer et al. (1995), used the description of angular momentum transport by Endal & Sofia. and investigated the evolution of rotation and lithium depletion. The model leads to a velocity in the inner parts of the Sun an order of magnitude too large than the observed value. Another problem arises from lithium abundances observations. They find that rotational mixing is necessary to explain lithium depletion in the Sun and young clusters, but they cannot reproduce the lithium dispersion observed in young clusters.

Zahn (1992) suggested that in addition to diffusive processes, meridian circulation, driven by solar-type wind, was at the origin of core angular momentum loss (see also Tassoul and Tassoul in a series of papers, 1995 and references therein). They treated meridian circulation as an advection process. Under the

assumption that angular velocity is a function of depth only, it is equivalent to an "hyper diffusion" process. But Matias & Zahn (1997) found that this process was not efficient enough to reproduce solar rotational profile at the age of the Sun.

Mestel, Tayler and Moss (1988) suggested that a primordial magnetic field would penetrate the core and enforce nearly uniform rotation along the field lines. Charbonneau and Mc-Gregor (1993) studied different poloidal field geometries and compared the velocity evolution inferred to a solar-type star spin-down on the main-sequence. Very different rotational evolutions are inferred from different field geometries. They found that a poloidal magnetic field geometry in which the magnetic field is restricted to the radiative parts leads to a velocity braking on the main sequence in agreement with the observations and is also in agreement with the internal rotational profile of the Sun. But there is no proof that such a configuration is stable and remains long enough to lead to an efficient braking.

Another process has been suggested to be at the origin of angular momentum extraction: internal (or gravity) waves (Press, 1981, Schatzman 1993). These waves, produced in the radiative zone by turbulent motions in the convective zone, would lead to an efficient braking of the core. Calculations suggest that angular momentum extraction in the solar interior would occur over a time scale of 10^7 yr (Zahn et al. 1997, Kumar & Quataert 1997).

In the past years, different models were developed to model the different processes that rule angular momentum evolution during PMS and MS.

McGregor & Brenner (1991) introduced a simple parameterized model of redistribution of angular momentum between the core and the envelope, both supposed to rigidly rotate to explain early MS evolution of solar-type stars. They found that a coupling time-scale of 10^7 yr was consistent with rapid spin-down of rapid rotators on the ZAMS.

Li & Collier Cameron (1993) investigated rotational evolution from ZAMS ages for solar-type stars. They supposed that the convective envelope applied a magnetic torque upon the – rigidly – rotating core: $T\alpha(\Omega_{conv} - \Omega_{rad})^\beta$. They found that only a weak coupling, characterized by a low value of the exponent β , and a large value of the ratio of the coupling time-scale to the braking time-scale was required to fit the observations of rapid rotators both in the Pleiades and Hyades clusters.

In another paper Collier Cameron and Li (1994) investigated the spin down of ZAMS stars without core-envelope decoupling – solid-body rotation – and found that appropriate Weber-Davis wind model combined with a simple linear dynamo which saturates at high rotation rates was also consistent with observations from ZAMS ages. They also introduce a mass-dependence of the saturation rate : higher masses require higher saturation rates.

Keppens et al. (1995) modeled evolution from T Tauri phase to MS. Their model treated angular momentum loss by a stellar wind, disk-locking, and angular momentum transport from the radiative interior to the convective envelope using McGregor & Brenner description. They found that a short coupling time of 10^7 yr and a dynamo saturated law for velocities larger than $\Omega = 20 \Omega_\odot$ were necessary to explain the large spread of velocities

among young clusters solar type stars, and rapid spin-down of rapid rotators on the ZAMS. They studied the evolution of a distribution at T Tauri ages with various assumptions in the initial velocity distribution, coupling time scale, and disk-lifetimes distribution. They found that the large velocity spread in young clusters could only be explained by an initial bimodal velocity distribution – the consequence of a bimodal disk lifetime distribution – and a mass spread, with 0.8 and 1 M_\odot stars in equal proportions. But at the age of Alpha Per and the Pleiades, observed proportion of slow rotators in the velocity range 0 – 10 km s^{-1} are 30% and 50% (respectively), while the model gives fractions lower than 5% in both clusters.

Barnes and Sofia (1996) focused on the existence of a population of ultra fast rotators among the young clusters Alpha Per and the Pleiades. They computed evolutionary models from T Tauri phases using a Kawaler-type braking law (see Sect. 3.2). They find that the Skumanich braking law ($\frac{d\Omega}{dt} \propto \Omega^3$) does not allow the existence of rapid rotators and investigated the effect of two different braking laws. The first one supposes a saturation of the momentum loss leading to a braking scaling as Ω , and the second suggests a change of the magnetic configuration from a dipolar form during pre-main sequence to a more solar form on the MS, and thus leads to a braking law scaling as Ω^2 . Comparisons with the observations of ultra-fast rotators tend to favor the first hypothesis, but they conclude that a combination of the two phenomena could be a better description of angular momentum evolution during pre-main sequence and main sequence phases. They also found that lower mass models require lower saturation thresholds.

In a recent paper, Krishnamurthi et al. (1997) investigated PMS and MS angular momentum evolution and compared solid-body models to models with internal differential rotation. They use the same diffusive processes as Chaboyer et al. (1995) for the treatment of angular momentum transport in the radiative parts. They find that a saturated braking law, with a mass-dependent value of the saturation rate is convenient to explain the mass dependence of the ultra-fast rotators (UFR's) phenomenon on the ZAMS. They conclude that the solid-body model requires a too large proportion of disks surviving longer than 20 Myr and thus, cannot reproduce the large proportion of slow rotators in young clusters, and that differential rotation is more convenient to reproduce the distributions of rotational velocities in young open clusters for masses in the 0.5 – 1.2 M_\odot range. They compare the fraction of slow rotators observed in Alpha Per and the Pleiades and find that there is a larger fraction of slow rotators in the latter. But they make their statistic with uncomplete sample and unresolved $v \sin i$ (Allain et al. 1997, Queloze et al. 1997a). They find that different disk-lifetimes distributions are required to fit the velocity distributions in different clusters and discuss the possibility of cluster-to-cluster intrinsic variations (e.g. of the initial conditions). They put a lower limit on the characteristic time-scale for core-envelope coupling of 70 to 100 Myr to explain the existence of a large proportion of slow rotators in young clusters.

Bouvier et al. (1997b) modeled the angular momentum evolution of stars in the mass range 0.5-1.1 M_\odot , during the PMS

and MS phases, with the assumptions of solid-body rotation, disk-locking and saturated wind braking law. They explore the evolution of a population of stars that appear in the T Tauri phase with a Gaussian-like period distribution. They show that solid rotation with a mass-dependent saturation rate, and a disk lifetime distribution which is a function of $\log(t)$, could reproduce the observed velocity distributions at different ages, and different masses. But the model did not try to reproduce the fraction of very slow rotators at ZAMS ages (with velocities lower than 5 km s^{-1}), nor its evolution on the main sequence. Finally, this model requires that 10% of the stars are still coupled to their disk at an age of 20 Myr, and that the maximum disk-lifetime be 40 Myr.

In this paper, I retain the same hypothesis of disk-locking but replace the solid-body assumption by a core-envelope decoupling hypothesis. I use the prescription by McGregor and Brenner: whatever may be the physical process of angular momentum transport in the radiative interior of the stars, it is supposed that the core rotates as a solid-body and that the exchanges between the radiative core and the convective envelope are controlled by a characteristic time-scale called coupling time, τ_c , introduced as a free parameter of the model. The coupling time τ_c is supposed to be constant all over the evolution of the star, from T Tauri phase, to the age of the Sun.

The aim of this paper is to investigate the effect of differential rotation on the angular momentum evolution of young low-mass stars. By this work, and in the light of new observational constraints, I wish to bring new insight on angular momentum transport processes, and especially on time scales involved in this processes.

In Sect. 2, I describe the constraints recent observations shed on rotation. In Sect. 3, I briefly describe the model and the different assumptions. In Sect. 4, I test the effects of the different parameters. and in Sect. 5, I investigate the specific effect of the coupling time, and present the evolution of a star of different masses, and different disk life times, for different coupling times.

2. Observational constraints

During the past years, many observational campaigns have been conducted to obtain new accurate measurements of the rotation rates of low mass stars of various ages. Efforts were made both to determine $v \sin i$ and rotational periods, and were especially conducted to determine *rotational velocities of slow rotators*, during pre-main sequence phase and in young clusters. For our computations I use a census of both $v \sin i$ and period determinations from various authors.

I divide our observational sample in three mass bins: 0.9 to $1.1 M_{\odot}$ stars are compared to $1 M_{\odot}$ model. 0.6 to $0.9 M_{\odot}$ stars are compared to 0.8 and $0.6 M_{\odot}$ models. And masses lower than $0.6 M_{\odot}$ are compared to $0.5 M_{\odot}$ model.

For T Tauri stars I used period determinations when available, or $v \sin i$ when star's radius is known (Bouvier et al. 1986, 1990, Hartmann et al. 1997, Hartmann & Stauffer 1989, Walter et al. 1988). In the case of T Tauri stars, the sample is too small

to be divided, and I use the same initial conditions over the full mass range. This leads to angular velocities for CTTS at the age of 10^6 yr , between 2 and $10 \Omega_{\odot}$, i.e 10 and 30 km s^{-1} .

Recent observations of post TTS (PTTS or naked TTS), discovered in the Chameleon and Lupus star forming regions from the ROSAT all-sky survey show a widening of the distribution of velocities with age (Wichmann et al. 1997, Covino et al, 1997, Bouvier et al. 1997a). The maximum velocity increases during the pre-main sequence and up to the arrival on the main-sequence (ZAMS). The PTTS cover an age spread between 1 Myr and a few 10 Myr. An interesting issue, in the case of PTTS, is the existence of a bias among X-ray selected observations against slow rotators, as activity is directly correlated to rotation. If this is the case, this bias would lead to an apparent lack of slow rotators during the PTTS phase. It is especially true for 0.6 to $0.9 M_{\odot}$ stars (see Fig. 13). How serious is this problem cannot be investigated for the moment, because of the pooriness of the sample of post-TTS for which $v \sin i$ is known.

Among young clusters there is a large dispersion of velocities: IC2602, IC2391 (30 Myr, Stauffer et al. 1997b), Alpha Persee (50 Myr, Prosser 1992, 1994, Stauffer et al. 1989, 1993), and the Pleiades (80-100 Myr, Soderblom et al. 1993, Queloz et al. 1997a, 1997b). In Alpha Per, velocities of $1 M_{\odot}$ stars extend from a few km s^{-1} up to 200 km s^{-1} , while in the Pleiades maximum velocity has decreased down to 50 km s^{-1} . In Alpha Per the fraction of very slow rotators ($v \sin i \leq 10 \text{ km s}^{-1}$) is around 30 % (Allain et al. 1997). In the Pleiades this fraction is $\simeq 50 \%$ (Allain et al. 1996).

M 34 (250 Myr, Jones et al. 1997), and M 7 (220 Myr Prosser et al. 1995) are intermediate clusters between the Pleiades and the Hyades ages (600 Myr, Radick et al. 1987, Stauffer et al. 1997c). On the main sequence, solar-type stars all have low rotation rates.

Important differences from one mass bin to another occur in young clusters and later. The time of the arrival on the main sequence depends on mass, and at the age of the M 34/M 7 clusters a one solar mass star is already on the main sequence, while a $0.5 M_{\odot}$ has just arrived on the ZAMS. In the Pleiades, the maximum velocity for $1 M_{\odot}$ stars is 50 km s^{-1} , while it is $100\text{-}150 \text{ km s}^{-1}$ for lower masses. The $v \sin i$ studies in this cluster show that the distribution of velocities is also mass-dependent: for spectral types later than G0, the minimum rotation rate increases with decreasing mass (Stauffer et al. 1997c). In the Pleiades cluster the proportion of stars with velocities lower than 10 km s^{-1} is about 35% for solar-mass stars, and is about 65% in the 0.6–0.9 mass range. (Allain et al, 1996, Queloz et al. 1997a, 1997b). In the cluster M 34, there is more spread in the velocities in the 0.6-0.9 M_{\odot} mass range than in the 0.9-1.1 M_{\odot} mass range ($7 - 45 \text{ km s}^{-1}$, $5 - 15 \text{ km s}^{-1}$, respectively). For the Hyades cluster, differences are even more striking and Radick et al. (1987) found a tight relationship between rotation period and mass down to $0.6 M_{\odot}$: the lower the mass, the lower the velocity. For masses lower than $0.6 M_{\odot}$, the Hyades stars still exhibit a dispersion of velocities comparable to the dispersion in M 34 for 0.6-0.9 M_{\odot} stars (Stauffer et al., 1997a), meaning that very low-mass stars still undergo a significant braking.

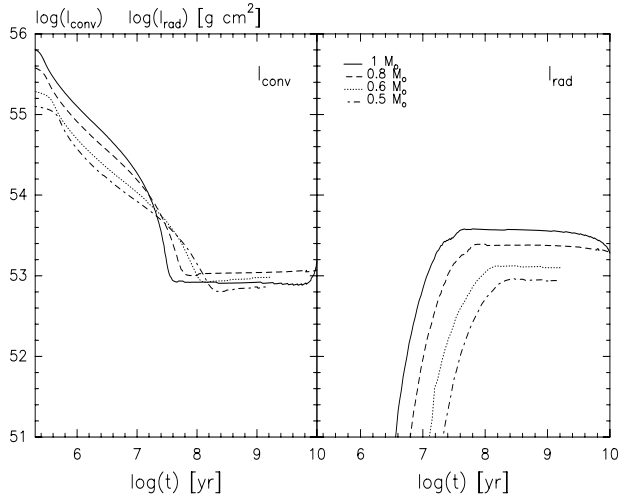


Fig. 1. Evolution of the moment of inertia for the core (right panel) and the envelope (left panel). Solid line is for $1 M_{\odot}$, dashed for $0.8 M_{\odot}$, dotted for $0.6 M_{\odot}$ and dotted-dash for $0.5 M_{\odot}$.

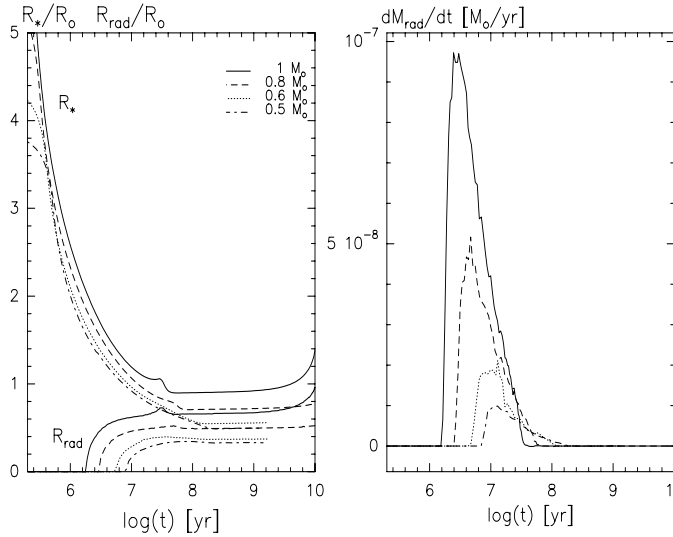


Fig. 2. Evolution of the star and core radius (left panel), and evolution of the mass variation of the core (right).

Most of the angular velocities presented here (see e.g Fig. 11) come from $v \sin i$ measurements, and are thus lower limits to the true angular velocities.

3. Description of the model

3.1. Evolutionary models

The evolutionary models for $1, 0.8, 0.6$ and $0.5 M_{\odot}$ have been computed by Forestini (1994). I refer to Bouvier (1997b) for details of the computation of the models. In Fig. 1 I present the evolution of the moment of inertia of both the core and the envelope for each model during the pre-main sequence phase of the star, and in Fig. 2 the evolution of the radii of the star and of the core (left panel), and the variation of the core's mass (right panel).

3.2. Hypotheses

The model is based on 3 assumptions: internal differential rotation, disk-locking and solar-type wind braking.

H1 differential rotation: it is assumed that the star rotates as a solid-body as long as it is completely convective. After the radiative core develops, the two zones will both rotate as solid-bodies with different angular velocities Ω_{rad} (for the core) and Ω_{conv} (for the envelope). Angular momentum exchanges between the two zones will then occur. Decoupling hypothesis is a reasonable compromise between solid-body models, and more physical models assuming local conservation of the angular momentum and transport processes in the radiative core.

The exchanges considered here have been described by MacGregor (1991) who suggested that a quantity ΔJ of angular momentum is extracted from the (fast) rotating core and is transferred to the (slower) envelope, and is defined by:

$$\Delta J = \frac{I_{conv} J_{rad} - I_{rad} J_{conv}}{I_{rad} + I_{conv}} \quad (1)$$

Where I_{rad} and I_{conv} are the moment of inertia for the radiative and convective zones respectively:

$$J_{conv} = I_{conv} \Omega_{conv} \quad J_{rad} = I_{rad} \Omega_{rad} \quad (2)$$

The quantity ΔJ is transferred over a time-scale τ_c , called coupling time, introduced as a free parameter of the model. If τ_c is short, the transfer of ΔJ would be almost instantaneous and would equilibrate Ω_{rad} and Ω_{conv} , leading to a quasi solid-body rotation.

Two main assumptions of the model presented here are thus that angular momentum exchanges are controlled by a coupling time, and that this coupling time has a fixed value and is not a function of mass, or core and/or envelope velocity, or any other parameter. This is probably a spurious assumption as there are some theoretical evidences that angular momentum transport depends on various physical characteristics of the star (core and/or envelope rotation, mass, depth of the convective zone...). In the case of angular momentum transfer by diffusive mechanisms, transport is a function of the velocity gradient inside the star. Krishnamurthi et al. (1997) modeled the angular evolution of young low-mass stars using angular momentum transport by hydrodynamics mechanisms and their time-scale for transport depends on the rotation rate (it is long for slow rotators and short for rapid rotators). Meridian circulation is induced by the angular momentum loss at the star's surface, and is thus a function of the surface velocity. In the case of internal waves extraction process, Zahn et al. (1997) found that the angular momentum flux depends linearly on the differential rotation.

It is the purpose of this paper to provide constraints on the coupling time, and eventually find a relationship with other stars parameters.

As the core grows, a quantity of material dM_{rad} , contained in a thin shell at a radius R_{rad} and with a velocity Ω_{conv} becomes radiative, (see Fig. 2) and the amount of angular momentum which is transferred from the envelope to the core during the

time interval dt is:

$$\frac{2}{3} R_{rad}^2 \Omega_{conv} \frac{dM_{rad}}{dt}$$

H2 Disk-locking: it is supposed that during the phase when the star accretes material from its surrounding disk, its surface rotational period remains constant. The theoretical basis for this assumption is the magnetic interaction between the star and its surrounding disk. Magnetic field lines shred the disk beyond the corotation radius, and tends to spin the central star down. The assumption that the stars accreting material from their surrounding disk are in a rotational equilibrium state, is supported by the observations of the rotation rates of both CTTS and WTTS. The latter tend to rotate faster than the former (Bouvier et al. 1993, Edwards et al. 1993, Choi & Herbst 1996). Computations from Königl (1991), Cameron & Campbell (1993), or Armitage & Clarke (1995) show that the star quickly reaches a constant angular velocity. This requires the existence of a stellar magnetic field of a few hundred Gauss (500 to 1000 Gauss typically), and accretion rates from 10^{-8} to $10^{-7} M_{\odot} yr^{-1}$. In this model it is supposed that as long as the star is accreting, its rotational period remains constant. From the moment the disk disappears, called disk lifetime, the star freely evolves.

H3 wind braking: The description used here is the description of angular momentum loss as described by Schatzman (1962), and parameterized by Kawaler (1988): angular momentum loss is a function of angular velocity, mass, mass loss and star radius.

$$\frac{dJ}{dt} = -K\Omega^{1+\frac{4an}{3}} \left(\frac{\dot{M}_{\star}}{M_{\odot}}\right)^{1-\frac{2n}{3}} \left(\frac{R_{\star}}{R_{\odot}}\right)^{2-n} \left(\frac{M_{\star}}{M_{\odot}}\right)^{-\frac{n}{3}} \quad (3)$$

The exponent n characterizes the field geometry, and a is the power of the linear dynamo relation $B\alpha\Omega^a$. I follow the suggestion by Kawaler and use $n = 1.5$, corresponding to an "intermediate" field geometry. As discussed by Charbonneau (1992), a braking-law with a fixed value of the exponent in the velocity term is unable to reproduce the standard model of angular momentum loss from Weber and Davis (1967). He pointed out that the WD model for slow rotators is well fitted with an exponent of 3 and the WD model for rapid rotators with an exponent of 2. Keppens et al. (1995) computed an angular momentum loss law from the WD solar wind model and also found that at low rotation rates the law is consistent with $\frac{dJ}{dt} \propto \Omega^3$ while for fast rotators it scales Ω^2 and Ω in the saturated regime. Barnes and Sofia (1996) also investigated the effect of different braking laws in order to reproduce the ZAMS ultra-fast rotators. They found that ultra-fast rotators could not be reproduced with a Skumanich-type braking law and thus required a change of the exponent at high velocities. They found that a saturated braking law with $\frac{d\Omega}{dt} \propto \Omega$ led to sufficiently high velocities. They also supposed a change of the magnetic configuration, from a more dipolar form during pre-main sequence to a solar-type form on the main sequence, that would lead to a PMS braking scaling Ω^2 .

Observational constraints for slow rotators comes from Skumanich's relation (1972): the velocity decrease of the MS slow

rotators is a power-law of the time $v\alpha t^{-\frac{1}{2}}$, where v represents rotational velocity. This relation leads to the braking law $\frac{dv}{dt} \propto v^3$. For rapid rotators, observations from Mayor and Mermilliod (1991) in young clusters lead to $\frac{dv}{dt} \propto v^2$.

In this paper, a Kawaler-type description of the braking law is used, with a three-part parameterization. Slow rotators follow the Skumanich regime, while intermediate rotators follow Mayor-Mermilliod regime. This is consistent with Barnes and Sofia assumption of a change of the magnetic configuration somewhere on the ZAMS, as intermediate rotators are mainly found during PMS. In addition it is supposed that saturation of the braking law occurs for high velocities, corresponding to a saturation of the dynamo-generated surface field for high velocities: $\frac{dv}{dt} \propto v$. These braking laws write:

$$\left. \frac{d\Omega_{conv}}{dt} \right|_{wind} = \frac{K_{sk}}{I_{conv}} \Omega_{conv}^3 \left(\frac{R_{\star}}{R_{\odot}}\right)^{\frac{1}{2}} \left(\frac{M_{\star}}{M_{\odot}}\right)^{-\frac{1}{2}}$$

Skumanich law: $\Omega_{conv} < \Omega_{crit}$, with $\Omega_{crit} = \frac{K_{mm}}{K_{sk}}$

$$\left. \frac{d\Omega_{conv}}{dt} \right|_{wind} = \frac{K_{mm}}{I_{conv}} \Omega_{conv}^2 \left(\frac{R_{\star}}{R_{\odot}}\right)^{\frac{1}{2}} \left(\frac{M_{\star}}{M_{\odot}}\right)^{-\frac{1}{2}}$$

Mayor-Mermilliod law: $\Omega_{conv} \geq \Omega_{crit}$ and $\Omega_{conv} < \Omega_{sat}$

$$\left. \frac{d\Omega_{conv}}{dt} \right|_{wind} = \frac{K_{mm}}{I_{conv}} \Omega_{conv} \Omega_{sat} \left(\frac{R_{\star}}{R_{\odot}}\right)^{\frac{1}{2}} \left(\frac{M_{\star}}{M_{\odot}}\right)^{-\frac{1}{2}}$$

Saturation: $\Omega_{conv} \geq \Omega_{sat}$

Three parameters are thus required to make a full description of the braking law: K_{sk} , K_{mm} and Ω_{sat} . In Sect. 4 I discuss how we constrain these parameters from the observations.

3.3. Equations of evolution

Using the above assumptions, equations of evolution for angular velocity write for the envelope:

if $t \leq t_{disk}$: $\Omega_{conv} = \Omega_0$

where Ω_0 is the initial velocity of the star.

if $t > t_{disk}$:

$$\frac{d\Omega_{conv}}{dt} = \frac{1}{I_{conv}} \frac{\Delta J}{\tau_c} - \frac{2}{3} \frac{R_{rad}^2}{I_{conv}} \Omega_{conv} \frac{dM_{rad}}{dt} - \left. \frac{\Omega_{conv}}{I_{conv}} \frac{dI_{conv}}{dt} - \frac{d\Omega_{conv}}{dt} \right|_{wind}$$

and for the core:

$$\frac{d\Omega_{rad}}{dt} = -\frac{1}{I_{rad}} \frac{\Delta J}{\tau_c} + \frac{2}{3} \frac{R_{rad}^2}{I_{rad}} \Omega_{conv} \frac{dM_{rad}}{dt} - \frac{\Omega_{rad}}{I_{rad}} \frac{dI_{rad}}{dt}$$

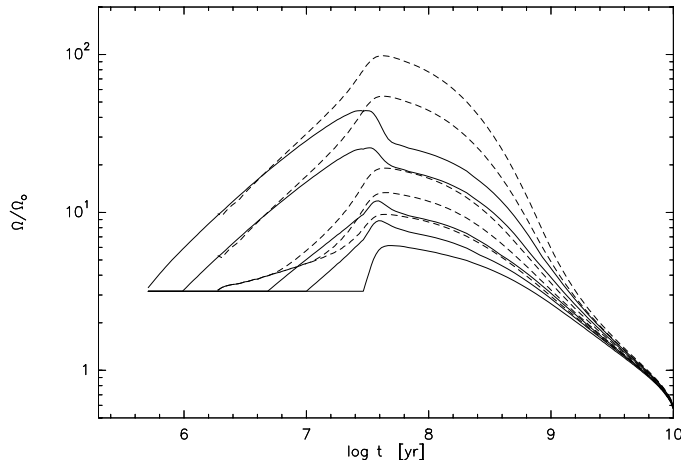


Fig. 3. Evolutionary tracks of a $1 M_{\odot}$ star for different disk lifetimes: 0.5, 1, 5, 10 and 30 Myr. Surface velocities are represented by solid lines and core velocities by dashed lines. Model is presented for a coupling time of $2 \cdot 10^7$ yr, $\Omega_{sat} = 30 \Omega_{\odot}$, $K_{sk} = 2.7 \cdot 10^{47}$ and $K_{mm} = 4.2 \cdot 10^{42}$.

4. Effects of varying the parameters

The evolution of a single star is submitted to 6 parameters related to the initial velocity, the disk lifetime, the wind braking law and the coupling time. In this section I present the effect of each parameter, independently of the value of the coupling time-scale. The effect of varying the coupling time is discussed in the next section.

4.1. Disk lifetime

The effect of the disk lifetime τ_{disk} for a $1 M_{\odot}$ star is presented on Fig. 3. The track for $\tau_{disk} = 0.5$ Myr corresponds to a star that loses its disk on the birth-line and, for a given initial velocity, sets an upper limit on velocities during the PMS and MS evolution. The 10 Myr and 30 Myr lifetimes set a lower limit on velocities and are used to compare the predictions of the different models for ZAMS slow rotators. The longer the disk-lifetime, the slower the rotator on the ZAMS. It is obvious for the surface velocity, but it is less obvious for the core velocity. The core appears with the same angular velocity than the envelope. If the disk still remains, the core immediately shows an acceleration, while the envelope keeps a constant angular velocity.

The disk-regulation nevertheless keeps the core from spinning up too quickly. From Eqs. 2, Eq. 1 writes:

$$\Delta J = \frac{I_{conv} I_{rad}}{I_{conv} + I_{rad}} (\Omega_{rad} - \Omega_{conv})$$

The angular momentum exchanges is a function of the difference of rotation between the core and the envelope, and as long as the star is coupled to the disk, the envelope keeps a very low rotation rate, leading to a large value of the quantity ΔJ , and thus a slower spin up of the core.

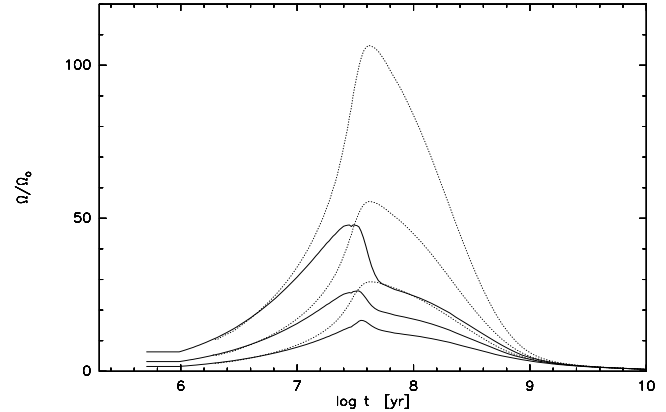


Fig. 4. Evolutionary tracks for the envelope (thick lines) and the core (dotted lines) velocities of a $1 M_{\odot}$ star for 3 different initial periods: $P_{init} = 4$ d (upper track), 8 d (middle track) and 16 d (lower track). See text for values of the parameters.

Therefore the disk-lifetime has an indirect consequence on differential rotation. On the other hand, the disk lifetime has no influence on MS velocities, past a few 10^9 yr, nor on the moment when convergence between the core and the envelope is reached.

4.2. Initial velocity

Classical T Tauri observations indicate that at an age of a few 10^6 yr, stars have rotational periods in the 4-16 days range with a peak around 8 days (see Sect. 2). This initial spread in velocities will remain at later ages. Fig 4 shows the evolution of a $1 M_{\odot}$ star that would appear in the T Tauri phase with an initial period of 4, 8 and 16 days. I present here velocities for radiative and convective zones in the case where the star would keep its accretion disk during 10^6 yr and for the following values of the model parameters: $\tau_c = 2 \cdot 10^7$ yr, $K_{sk} = 2.7 \cdot 10^{47}$, $K_{mm} = 4.2 \cdot 10^{42}$, and $\Omega_{sat} = 30 \Omega_{\odot}$.

A difference in the initial velocity remains all over the PMS and early MS evolution. A star that would have an initial velocity twice as large as another, will rotate twice as fast during the entire PMS phase. On the other hand, initial velocity has no influence upon the final velocity when MS braking is achieved, in other words, the MS star does not keep memory of its initial velocity. Initial velocity has no influence either on differential rotation: the core velocity varies in the same way the surface velocity does, and the time when convergence is attained does not change.

Effects of different initial velocities can be distinguished from the effects of different disk lifetimes for slow rotators only. More precisely, if the disk disappears before the core develops, evolutionary tracks look exactly the same in both cases. Difference occurs when the disk survives after the core has developed because the envelope keeps a constant period while the core spins up. In the case of different initial periods, even for slow rotators the core and the envelope both spin up.

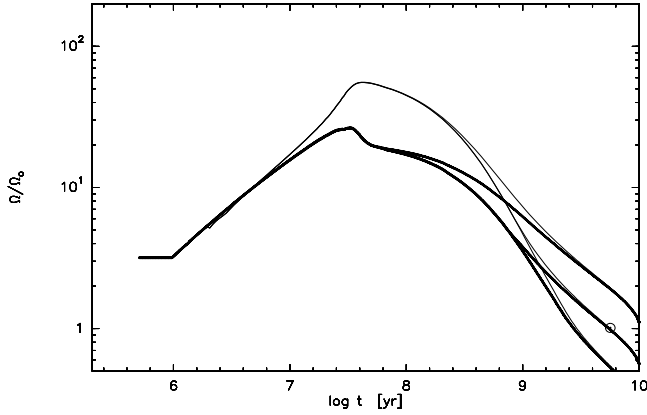


Fig. 5. Evolutionary tracks of a $1 M_{\odot}$ star for 3 different values of the parameter K_{sk} : $7.5 \cdot 10^{46}$ upper track, $3 \cdot 10^{47}$ is middle track, and $1.2 \cdot 10^{48}$ is lower track. Tracks for the envelope are thick lines, and for the core are thin lines. The correspondent values of Ω_{crit} are 19.5, 4.9 and $1.2 \Omega_{\odot}$.

4.3. The braking law

As described in the previous section, 3 parameters are used to describe the magnetic braking law: K_{sk} , the constant for slow rotators, K_{mm} , for intermediate rotators, and Ω_{sat} , the rotational value of the saturation. The value of the rotation rate at which braking goes from the Skumanich regime to the Mayor-Mermilliod regime is defined by: $\Omega_{crit} = \frac{K_{mm}}{K_{sk}}$.

Fig. 5 shows the influence of the constant of the Skumanich's law for slow rotators, K_{sk} , for the core and the envelope. Three different values are presented: $7.5 \cdot 10^{46}$, $3 \cdot 10^{47}$ and $1.2 \cdot 10^{48}$. The values of the other parameters are $K_{mm} = 4.2 \cdot 10^{42}$, corresponding to $\Omega_{crit} = 19.5, 4.9, \text{ and } 1.22 \Omega_{\odot}$, and $\Omega_{sat} = 30 \Omega_{\odot}$. The effect of K_{sk} is concentrated on slow rotators on the MS for both the envelope and the core velocities. The value of K_{sk} , by influencing the value of Ω_{crit} , influences the moment the tracks enter the Skumanich's regime on the main sequence. Thus, the lower K_{sk} the weaker the braking law on the main sequence, and the earlier the star enters the Skumanich's regime. Both effects contribute to a weaker braking of the slow rotators.

The other parameters are the constant of the braking law which applies for moderate rotators K_{mm} , and the value of the rotation rate at which saturation occurs Ω_{sat} . To investigate the effect of Ω_{sat} I take extreme values: 5.5, 30 and $60 \Omega_{\odot}$. For the lower saturation rate the braking goes from the Skumanich regime to the saturated regime with no intermediate Mayor-Mermilliod regime. For the higher rotation rate the stars are most of the time in the Mayor-Mermilliod regime. Fig. 6 presents 3 tracks corresponding to three different values of the disk lifetime: 0.5, 10 and 30 Myr. The values of the other parameters are $\tau_c = 2 \cdot 10^7 \text{ yr}$, $K_{sk} = 2.7 \cdot 10^{47}$, $K_{mm} = 4.2 \cdot 10^{42}$ ($\Omega_{crit} = 5.4 \Omega_{\odot}$). The effect of the parameter Ω_{sat} is concentrated on rapid rotators for high saturation values and affects slow rotators for low Ω_{sat} only. As for K_{sk} the effect is essentially sensitive between 10 and 100 Myr, i.e. from ZAMS ages. The lower the saturation rate the weaker the braking law and the higher the rotation on the ZAMS. For $\Omega_{sat} = 60 \Omega_{\odot}$, the max-

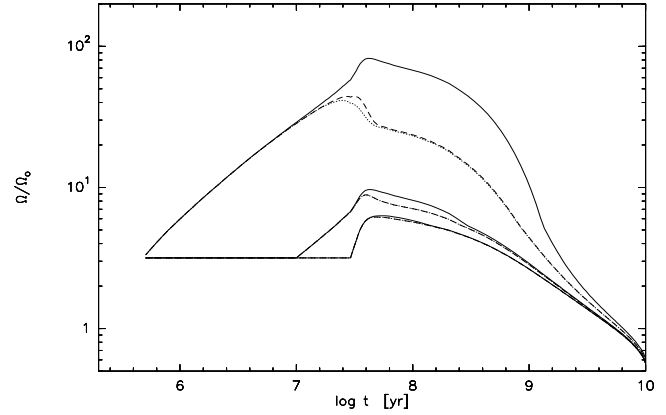


Fig. 6. Evolutionary tracks of a $1 M_{\odot}$ star for 3 different values of the parameter Ω_{sat} : $5.5 \Omega_{\odot}$ is solid line, $30 \Omega_{\odot}$ is dashed line, and $60 \Omega_{\odot}$ is dotted. See text for values of the parameters.

imum velocity is only $50 \Omega_{\odot}$, so the saturation value is never reached. For long disk lifetimes $\Omega_{sat} = 30$ and $60 \Omega_{\odot}$ tracks are superimposed: the saturation value is never reached, and hence the braking law is the same for both tracks. In addition of changing the maximal value reached on the ZAMS, a difference in Ω_{sat} changes the moment when this maximum is reached: the lower Ω_{sat} the later the braking occurs. Furthermore, the effect of a weaker braking law is also seen during early MS, where it is more difficult to brake ZAMS ultra fast rotators (UFR's).

Early pre-main sequence evolution (before 10 Myr) is independent of the value of Ω_{sat} as the evolution during this phase is completely dominated by the contraction effects. Finally, the final velocity, at 10^{10} yr , is not dependent on Ω_{sat} .

Now, to investigate the effect of K_{mm} , Ω_{sat} is set to $300 \Omega_{\odot}$, so that the saturation value is never reached, and the star is most of the time in the Mayor-Mermilliod regime. The evolutionary tracks are presented for 3 values of K_{mm} : $1.05 \cdot 10^{42}$, $4.2 \cdot 10^{42}$ and $1.68 \cdot 10^{43}$ ($\Omega_{crit} = 1.36, 5.42 \text{ and } 23.05 \Omega_{\odot}$ respectively, see Fig. 7). τ_c is set to $2 \cdot 10^7 \text{ yr}$ and $K_{sk} = 2.7 \cdot 10^{47}$. The value of K_{mm} affects tracks for both rapid and slow rotators. The lower K_{mm} , the higher the velocity on the ZAMS, and the later the braking. Differences in the tracks remain during early phases of the main sequence and progressively disappear. The rotation rate at the age of the Sun still slightly depends on the value of K_{mm} .

The values of the braking law parameters can be constrained by the observations: as K_{mm} and Ω_{sat} poorly affect the tracks for slow rotators on the main sequence K_{sk} is completely determined by the solar calibration of the model. And a combination of the two parameters K_{mm} and Ω_{sat} is determined to fit both rapid rotators on the ZAMS, and their rapid braking on the early MS.

5. Core-envelope decoupling

In this section I present the effects of the choice of the coupling time on the evolutionary tracks of a single star. The results of the model are presented for four different masses: 1, 0.8, 0.6

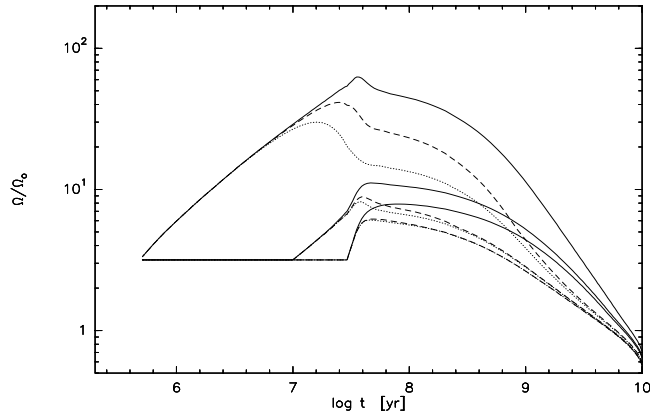


Fig. 7. Surface rotation evolutionary tracks of a $1 M_{\odot}$ star for 3 different values of the parameter K_{mm} : $K_{mm} = 1.05 \cdot 10^{42}$ ($\Omega_{crit} = 1.4 \Omega_{\odot}$) is solid line, $4.2 \cdot 10^{42}$ ($\Omega_{crit} = 5.4 \Omega_{\odot}$) is dashed line for, and $1.68 \cdot 10^{43}$ ($\Omega_{crit} = 23.0 \Omega_{\odot}$) dotted. See text for values of the parameters.

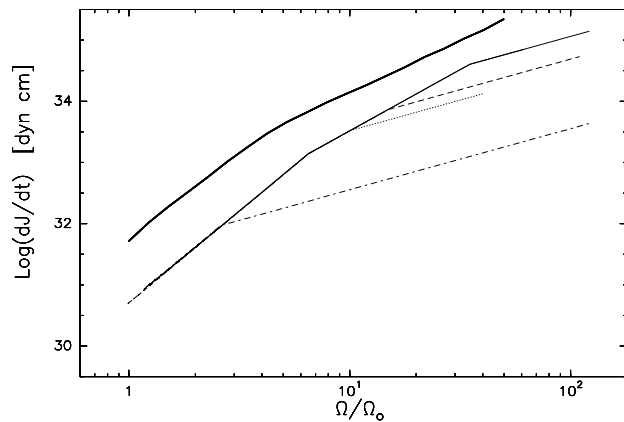


Fig. 8. Braking law for the short coupling time model, $\tau_c = 10^6$ yr. solid line is for $1 M_{\odot}$, dashed is for $0.8 M_{\odot}$, dotted for $0.6 M_{\odot}$ and dash-dotted for $0.5 M_{\odot}$. The thick solid line represents Charbonneau's braking law (1992) computed from Weber-Davis model. Values of the parameters are $K_{sk} = 2.25 \cdot 10^{47}$, $K_{mm} = 4.2 \cdot 10^{42}$ and $\Omega_{sat} = 35, 15, 10, 2.6 \Omega_{\odot}$, for $1, 0.8, 0.6$ and $0.5 M_{\odot}$, respectively.

and $0.5 M_{\odot}$. The braking laws are presented for the different models and the different masses in Figs. 8, 9 and 10 where the angular momentum loss is presented as a function of the angular velocity. The braking law computed by Charbonneau (1992) from Weber & Davis model is also plotted. For the three coupling time models presented here, the braking rates are always lower than the braking rate predicted by the Weber-Davis wind model.

5.1. Choice of the coupling time τ_c

Evolutionary tracks are presented for 3 different coupling times: 10^6 yr, which I will call “short”, $2 \cdot 10^7$ yr, will be called “intermediate”, and $5 \cdot 10^8$ yr, will be called “long”. Choices of the coupling times are dictated by both theoretical and observational reasons. The short coupling time is short enough compared to the evolutionary time-scales (contraction, nuclear), so

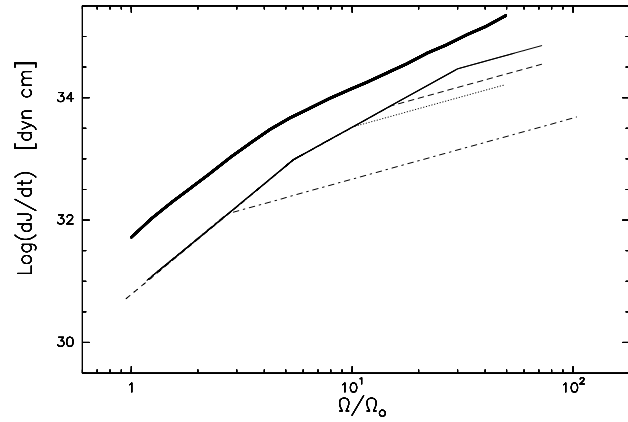


Fig. 9. Same as Fig. 8 for the intermediate coupling time model, $\tau_c = 2 \cdot 10^7$ yr, and with $K_{sk} = 2.7 \cdot 10^{47}$, $K_{mm} = 4.2 \cdot 10^{42}$ and $\Omega_{sat} = 30, 15, 10, 2.7 \Omega_{\odot}$.

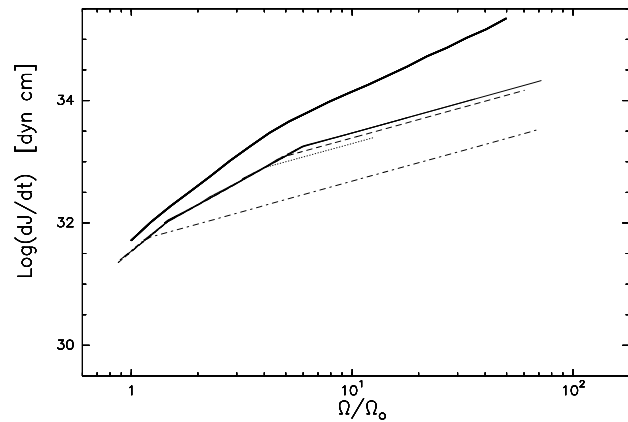


Fig. 10. Same as Fig. 8 for the long coupling time model, $\tau_c = 5 \cdot 10^8$, and with $K_{sk} = 1.5 \cdot 10^{48}$, $K_{mm} = 6.3 \cdot 10^{42}$ and $\Omega_{sat} = 6, 5, 4, 1.2 \Omega_{\odot}$.

that the star can almost be considered as rotating as a solid-body. The long coupling time (corresponding to almost the age of the Hyades cluster) is far longer than other time scales involved in PMS evolution, so that at the arrival on the MS, stars in clusters like Alpha Per and the Pleiades can be considered as totally decoupled. Finally, I chose an intermediate coupling time which corresponds to the maximal coupling-time required to have a $1 M_{\odot}$ star in quasi solid-body rotation at the age of the Sun. Each model was calibrated so that $1 M_{\odot}$ tracks fit the solar value at the age of the Sun, and are therefore submitted to different braking laws. For a given model, braking law parameters K_{sk} , K_{mm} and Ω_{sat} were chosen as the best fit of the observations for $1 M_{\odot}$ over the complete evolutionary time interval considered here: from 1 Myr to the age of the Sun. And for other masses we scale the value of the saturation parameter Ω_{sat} . In all models, the lower the mass, the lower the saturation value (see Figs. 8, 9 and 10).

Each model is discussed with three different disk lifetimes: $5 \cdot 10^5$, 10^7 and $3 \cdot 10^7$ yr, for 1 and $0.5 M_{\odot}$, and $3 \cdot 10^5$, 10^7 and $3 \cdot 10^7$ yr, for 0.8 and $0.6 M_{\odot}$. The first disk lifetime represents a star which would lose its disk almost on the birth-line. Thus, for a given set of parameters (initial period, braking law) it

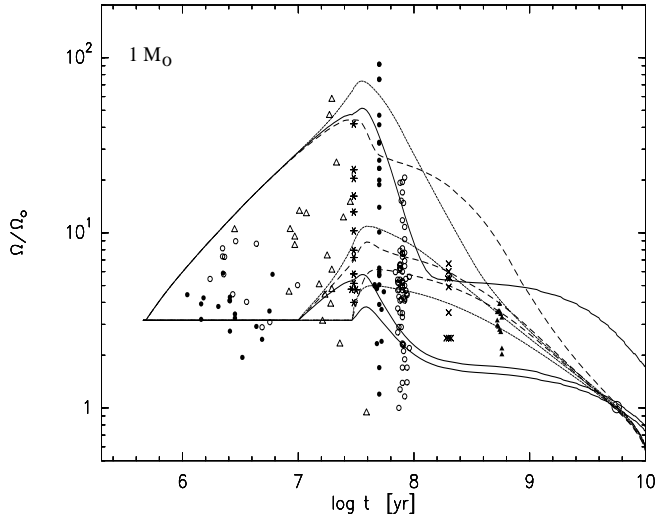


Fig. 11. Angular surface velocity evolutionary tracks for a single star of $1 M_{\odot}$ are represented for an initial period of 8 d and 3 different disk lifetimes: 0.5, 10 and 30 Myr. Dotted line is for $\tau_c = 10^6$ yr, dashed line is for $\tau_c = 2 \cdot 10^7$ yr and solid line for $\tau_c = 5 \cdot 10^8$ yr. Observations are presented with different symbols: filled dots during PMS are CTTS, empty dots are WTTS. Empty triangles are PTTS, stars are IC2602 and IC2391. Filled dots on the ZAMS are Alpha Per, empty dots are the Pleiades. Crosses are M 34. Filled triangles are the Hyades, and the Sun is a dotted circle.

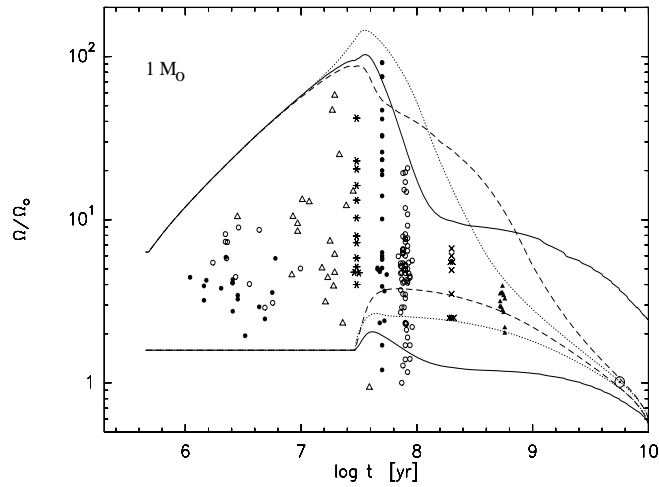


Fig. 12. Angular surface velocity evolutionary tracks for a single star of $1 M_{\odot}$, for the coupling time scales presented in Fig. 11, and 2 different initial period. Upper tracks are initial period of 4d and lower tracks are 16d

can be considered as an upper limit to the velocities during the evolution. Four different masses are also represented: $1 M_{\odot}$ in Fig. 11, $0.8 M_{\odot}$ in Fig. 13, $0.6 M_{\odot}$ in Fig. 14, and $0.5 M_{\odot}$ in Fig. 15. Finally, models for 0.5, 0.6, 0.8 and $1 M_{\odot}$ are presented with an initial period of 8 days, which is the mean observed period during Classical T Tauri phase. For $1 M_{\odot}$ models evolutionary tracks are also plotted using initial periods of 4 and 16 days, which correspond to minimum and maximum periods found among T Tauri stars (Fig. 12).

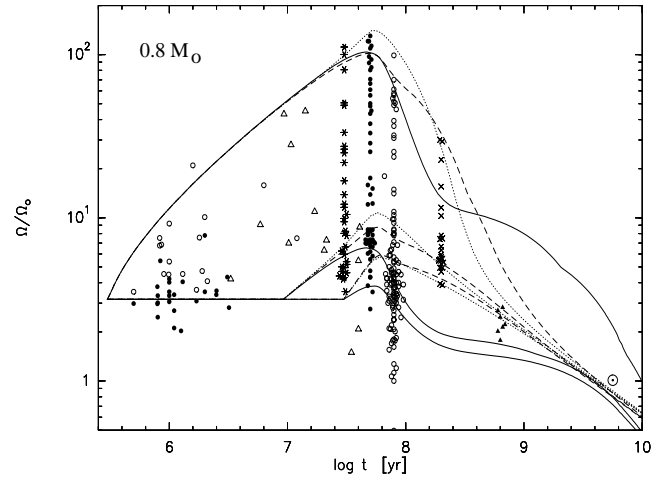


Fig. 13. Same as Fig. 11 for $M=0.8 M_{\odot}$.

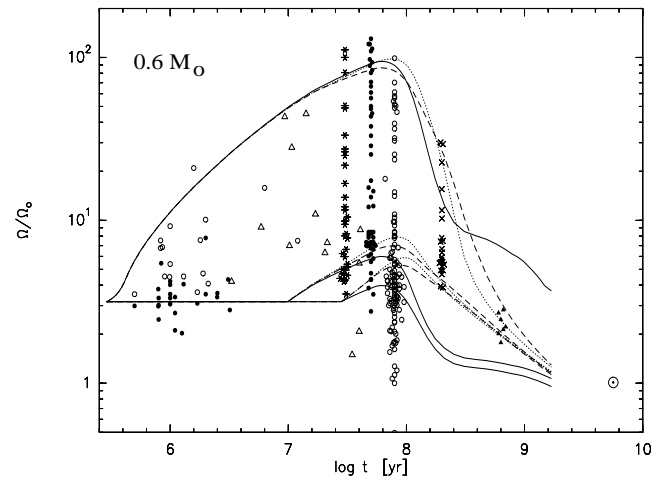


Fig. 14. Same as Fig. 11 for $M=0.6 M_{\odot}$

5.2. Short coupling time

In Figs. 11, 13, 14 and 15, the $\tau_c = 10^6$ yr model is represented by dotted lines. This model is very close to a solid-body model, as angular momentum transport occurs upon a time-scale far shorter than evolutionary time-scales. For the $1 M_{\odot}$ model, solar calibration leads to $K_{sk} = 2.25 \cdot 10^{47}$, and the best fit of the observations is obtained for $K_{mm} = 4.2 \cdot 10^{42}$ and $\Omega_{sat} = 35 \Omega_{\odot}$. With this model it is very easy to account for ultra fast rotators during PMS and ZAMS phases. The largest velocity is more than $70 \Omega_{\odot}$ ($\sim 140 \text{ km s}^{-1}$), and the more rapid rotator in the 0.9-1.1 M_{\odot} mass range in Alpha Per has $100 \Omega_{\odot}$ ($\sim 200 \text{ km s}^{-1}$). Then, from ZAMS ages the stars are rapidly braked. At the age of the Pleiades the largest velocity is however larger than the velocity observed ($40 \Omega_{\odot}$ vs $20 \Omega_{\odot}$). This suggests that the spin-down is not strong enough to reproduce the upper limit of velocities both in the Alpha Per and the Pleiades clusters. The rapid braking of rapid rotators requires a strong braking rate for high velocities, which requires a high value of the saturation rate ($\Omega_{sat} = 35 \Omega_{\odot}$). A stronger braking law would lead to lower

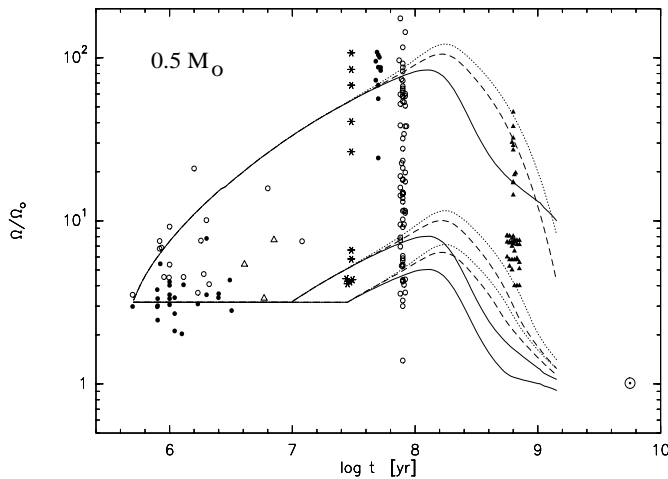


Fig. 15. Same as Fig. 11 for $M=0.5 M_\odot$

velocities at the age of Alpha Per . It is however not clear that the age of the Pleiades is 80 Myr, as it is presented here. It has been claimed that the Pleiades were older (about 100 Myr) and some authors even find that the Pleiades cannot be younger than 130 Myr (Basri et al. 1997). If the Pleiades cluster is 100 Myr or more, the short coupling time model leads to a better agreement with the observations of maximum velocities: the track with an initial period of 8 days has an angular velocity of $20 \Omega_\odot$ at 130 Myr.

At the age of the Hyades, all stars have converged to low angular velocity rates between 2 and 3 times the solar value, in accordance with the observations. And braking extends up to the age of the Sun. Observed braking of rapid rotators is thus roughly reproduced from the ZAMS up to the age of the Sun.

Because the only process that keeps the stars from spinning up is the disk-locking, the slow rotators at ZAMS ages and during the early MS are more difficult to account for. The angular momentum losses by magnetic wind occur over a longer time-scale, and are therefore inefficient during the PMS phase. It is then necessary to suppose that the disk-regulating is effective up to at most 30 Myr (Bouvier et al. 1997b for a discussion). A 10 Myr disk lifetime leads to a velocity of 20 km s^{-1} at the Pleiades' age (we take the Pleiades age to be 80 Myr, Fig. 11), and a 30 Myr disk leads to $v = 9\text{-}10 \text{ km s}^{-1}$. Of course a longer period leads to a lower velocity at ZAMS ages and a star that would keep its disk 30 Myr, with an initial period of 16d, arrives on the ZAMS at 4 km s^{-1} .

In the Pleiades a large proportion of stars (about 50 %) have $v \sin i$ lower than 10 km s^{-1} . The solid-body model then requires that a large fraction of stars have long-lived disks. But the fraction of long disk lifetimes can be substantially reduced if we take into account the effect of the $\sin i$ distributions. The contamination by $\sin i$ factor is very important in the Pleiades cluster as all the stars are slow or moderate rotators. The mean value of $\sin i$ is $\pi/4$, so that stars with true velocities between 10 and 13 km s^{-1} will on average have $v \sin i$ to the range $8\text{-}10 \text{ km s}^{-1}$. $\sin i$ contamination is a statistical effect, and there

probably is some stars with very low velocities, but the true fraction of slow rotators is lower than the observed fraction. Recent $v \sin i$ measurements in the Pleiades cluster (Queloz et al. 1997a, 1997b) suggest that the fraction of true velocities lower than 10 km s^{-1} is $\simeq 35 \%$ for solar-type stars, thus lower than the fraction of $v \sin i$.

Bouvier et al. (1997b) suggested that the initial distribution of period at T Tauri ages is well fitted with a Gaussian curve with a mean period of 8 d. In their model, with a disk lifetime of 10 Myr, a star with an initial period of 8 d reaches the age of the Pleiades with a velocity of 10 km s^{-1} . It thus requires that 35 % of the stars keep their disk longer than 10 Myr in order to reproduce the 35 % of slow rotators. In their paper Bouvier et al. summarize the different PMS disks observations and surviving disk fractions estimations at different ages. At the moment, and without taking into account PMS stars dispersed in star forming regions recently discovered by ROSAT, the fraction of stars still surrounded by a disk at an age of 10 Myr is 10 to 30 % (Strom et al. 1995, Lawson et al. 1996). It thus seems difficult to explain that 35 % of the stars have rotational velocities lower than 10 km s^{-1} at the age of the Pleiades. In the present model (Fig. 11), stars which decouple from their disk at an age of 10 Myr reach the age of the Pleiades with a velocity of 20 km s^{-1} . Such a difference with Bouvier et al. model can be explained by a difference in the braking law. In that case, it is even more difficult to explain the large fraction of slow rotators on the ZAMS.

By the time the stars arrive on the ZAMS, at the Alpha Per cluster age, the slow rotators are submitted to a weak braking with the short coupling time model. It is very difficult indeed to slow down slow rotators if we consider solid-body rotation, because the braking applies on the entire star. The consequence is that between the age of the young clusters IC2391 and IC2602 (30 Myr) and the age of the Pleiades, the slow rotators – below 10 km s^{-1} – should keep roughly the same velocity. In other words, the proportion of very slow rotators in these clusters must be roughly the same. This point will be discussed in Sect. 6.

$0.8 M_\odot$ and $0.6 M_\odot$ models require, respectively, $\Omega_{\text{sat}} = 15$ and $10 \Omega_\odot$ to account for fast rotators in young clusters (Fig. 13 and 14). For both 0.8 and $0.6 M_\odot$, rapid rotators and their braking during the main sequence, are well fitted. As for $1 M_\odot$ stars a large fraction of stars are slow rotators.

At later ages on the MS, the short coupling time models find that the lower the mass, the lower the velocity. The braking law was chosen so that the $1 M_\odot$ model fits the solar value. For $0.8 M_\odot$ model, velocities at the age of the Sun are between 0.8 and 0.9 the solar value. For $0.6 M_\odot$, evolutionary tracks stop before reaching solar ages, but from the position of the tracks at the Hyades age, $0.6 M_\odot$ model should reach lower values than the $0.8 M_\odot$ model. This point is thus in agreement with the observations in the Hyades cluster.

The velocity distributions for $0.5 M_\odot$ stars show significant differences with other masses in young clusters like Pleiades and Alpha Per, and for evolved ones like Hyades. In the former, the distributions are quite flat – there is no peak of the distribution for slow rotators – and for the latter, rapid rotators

(with velocities up to 25 km s^{-1}) still exist. These distributions are well fitted with a short coupling time model with $\Omega_{sat} = 2.6 \Omega_{\odot}$, which means that braking goes from Skumanich's law to saturated regime, with no intermediate Mayor-Mermilliod regime. Velocity braking occurs at 150-200 million years, and is not achieved at the age of the Hyades. It also means that at the age of the Pleiades, maximum is not attained, and $0.5 M_{\odot}$ stars have not reached the ZAMS.

With 0.5 and $0.6 M_{\odot}$ models it is more difficult to account for rapid rotators in young clusters than with 0.8 and $1 M_{\odot}$ models. A larger initial velocity would however account for rapid rotators.

In conclusion, the main problem for the solid-body model is the existence of numerous slow rotators in young clusters. This might not really be a problem if these slow rotators are *sini* contaminated. Precise determinations of the true slow rotators fraction, both at the Alpha Per cluster and the Pleiades ages are required to answer the question whether solid-body model, with a realistic disk lifetimes distribution, can reproduce the slow rotators observations.

5.3. Intermediate τ_c

In Figs. 11, the intermediate τ_c model is represented by dashed lines. I find the best model to have nearly the same braking law as the short coupling time model: $K_{sk} = 2.7 \cdot 10^{47}$, $K_{mm} = 4.2 \cdot 10^{42}$ and $\Omega_{sat} = 30 \Omega_{\odot}$. A weaker braking law would lead to faster rotators on the ZAMS, but would also lead to faster rotators on the MS. The rapid braking phase is very short, and rapid rotators are not significantly braked between Alpha Per and the Pleiades.

What makes a rapid spin-down so difficult to obtain is that with $\tau_c = 2 \cdot 10^7$ yr, angular momentum transfer from the core to the envelope begins at ages typically between those of the clusters IC2602/2391 and Alpha Per. This makes braking very inefficient during the early stages of MS as the rate of angular momentum transferred from the core to the envelope compensates the loss of angular momentum from a magnetic wind. This leads to a plateau of the rotation curve between 70 Myr and 250 Myr. On the other hand, with a stronger braking law, it would be impossible for the stars to reach high velocities of 200 km s^{-1} on the ZAMS. The best braking law is then a compromise between the existence of fast rotators and rapid spin-down of these rotators.

With this model very slow rotators are even more difficult to account for than with the short coupling time model. With a disk lifetime of 30 Myr, the short τ_c model leads to velocities of 10 km s^{-1} on the ZAMS (Fig. 11), while the intermediate τ_c model leads to a larger value of the rotation rate of 12 km s^{-1} . This can be explained as follows: after 30 Myr, angular momentum transfer from the core to the envelope for the intermediate coupling time model is in progress, thus leading to higher values of the rotation rate. It is the opposite if we consider the tracks with a disk lifetime of 10 Myr: the short coupling time model leads to higher velocities than the intermediate model. This difference between the two disk lifetimes tracks can be explained

by core-envelope decoupling effects: between 10 and 30 Myr, the angular momentum transfer from the core to the envelope is not yet effective and braking is more efficient for the de-coupled model.

With the intermediate coupling time model angular momentum transfer is really effective between a few 10 Myr and a few 100 Myr, so that braking nearly stops (this effect is especially important for solar-type stars). At later ages, minimum velocities reached for clusters M 34 and Hyades are too large compared to observed velocities. And maximal velocities are as well far too large.

On the other hand, for a coupling time of $2 \cdot 10^7$ yr, stars at the age of the Sun have all been braked to a few km s^{-1} , and rotate almost like solid-bodies. This coupling time model is therefore able to reproduce the solar rotation profile, while a longer coupling time would lead to differential rotation for solar-type stars at solar age (see Sect. 5.4)

For 0.8 and $0.6 M_{\odot}$ models Ω_{sat} is set to 15 and $10 \Omega_{\odot}$, respectively (Fig 13 and 14). For slow rotators there is no significant difference between the short and the intermediate models. For $0.6 M_{\odot}$ models there are much less differences between short τ_c model and the intermediate coupling model than for $1 M_{\odot}$ tracks. More precisely, the two models find almost the same velocities for highest and slowest rotators in clusters Alpha Per, the Pleiades, M 34 and even Hyades. There are two possible explanations to this. First, for $0.6 M_{\odot}$ stars, the evolutionary time is longer than for higher masses, and longer than the intermediate coupling time of $2 \cdot 10^7$ yr presented here. In that case, this model acts nearly as a solid-body model. Opposite to higher masses, this model leads to rotations rates lower than the short coupling time in the last evolutionary track – with $\tau_{disk} = 30$ Myr. As the MS is not reached yet, spin-up from contraction remains the main process that controls the angular momentum evolution, and is more efficient in the case of solid-body rotation. Second, the lower the mass, the smaller the radiative core. The role of the core –a reservoir of angular momentum– is thus less important for lower masses as for higher masses. Therefore, inferred differential velocity is also less important.

For masses lower than $0.6 M_{\odot}$, Ω_{sat} is set to $2.7 \Omega_{\odot}$. As for $0.6 M_{\odot}$ models, evolutionary tracks for this model are not significantly different from the short coupling time model. The slight difference is explained by different braking laws. The plot of the core velocity shows that the intermediate coupling time model acts like a solid model for $0.5 M_{\odot}$ (see previous section).

With this model, the coupling time is short enough to reproduce the solar rotational profile. But at least for $1 M_{\odot}$ stars, it is difficult to account for 1) the existence of UFR's on the ZAMS, and, 2) the rapid spin-down of these UFR's at the age of the Pleiades, 3) the important spin-down down to a few km s^{-1} at the age of the Hyades and 4) slow rotators at the early stages of the main sequence evolution. For low masses of 0.5 and $0.6 M_{\odot}$, this model behaves almost like a solid-body model, and leads to a good agreement with the observations.

In their model, Keppens et al. claimed that a coupling time of $\tau_c = 10$ Myr is able to reproduce the observed velocity distributions at different ages, from the T Tauri phase up to the

age of the Sun. From the work presented here, a model with a coupling time of 20 Myr leads to important differences with the observations. Differences in the assumptions of the models lead to differences in the resulting angular momentum evolution. Keppens et al. used an initial distribution mixing 0.8 and $1.0 M_{\odot}$ stars. But there are important differences between the 0.8 and $1 M_{\odot}$ observed velocity distributions, especially in the Pleiades, where solar-mass stars all have velocities lower than 60 km s^{-1} while the largest observed velocity among $0.8 M_{\odot}$ is larger than 100 km s^{-1} (Queloz et al. 1997). So the important braking observed for solar-type stars between the age of Alpha Per and the age of the Pleiades is not reproduced by their model. Furthermore, they artificially increase the number of very slow rotators among solar-type stars, as $0.8 M_{\odot}$ stars are more easily braked than $1 M_{\odot}$. Finally, even with adding $0.8 M_{\odot}$ stars to their sample, they obviously cannot reproduce the large number of stars with velocities lower than 10 km s^{-1} on the ZAMS. The maximum disk lifetime they use is 6 Myr, but even if they use a longer disk lifetime, they cannot produce more very slow rotators. From the tracks presented on Fig. 3, the longest disk lifetime (30 Myr) leads to a minimal velocity on the ZAMS of 10 km s^{-1} , while a disk lifetime of 1 Myr leads to a velocity of 20 km s^{-1} . It is thus easy to reproduce velocities in the range $10\text{-}20 \text{ km s}^{-1}$ on the ZAMS with an intermediate coupling time model. It is indeed the result found by Keppens et al., as at the Pleiades age, 60% of the stars are in this velocity range.

5.4. Long τ_c

For this model, solar calibration leads to $K_{sk} = 1.5 \cdot 10^{48}$, and I use $K_{mm} = 6.3 \cdot 10^{42}$ and $\Omega_{sat} = 6 \Omega_{\odot}$. A coupling time of $5 \cdot 10^8 \text{ yr}$ is far longer than PMS evolutionary times of the $1 M_{\odot}$ stars. The core and the envelope are then completely decoupled up to a few 100 Myr, i.e., far after the star has reached the age of the Pleiades. As only the convective envelope is subject to wind braking it is very easy to keep slow rotators at T Tauri ages slowly rotating up to the age of the Hyades. From the moment the star stops its contraction it is significantly braked.

For rapid rotators, this decoupling leads to a very efficient braking between the age of Alpha Per and the age of the Pleiades, more efficient than in the case of solid-body model. This rapid braking is indeed required to account for the decrease of velocities of the most rapid rotators in both clusters. During the same time scale slow rotators are also braked: a star with a velocity of 5 km s^{-1} in Alpha Per has a velocity of 3 km s^{-1} in the Pleiades. In that case, a disk lifetime value of 10 Myr is sufficient to account for velocities as low as 5 km s^{-1} at the age of Alpha Per and 3 km s^{-1} in the Pleiades.

While the spin-down is consistent with the observations during the early MS phases, it is less efficient on the MS at later ages because by an age of a few 10^8 yr angular momentum transfer from the core to the envelope becomes effective. A spread in the velocities then remains during MS. A spread in the velocities is really observed in the old clusters M 34 and the Hyades, but the model cannot reproduce the decrease of the maximum velocity between these two clusters, as the model predicts more

a plateau than a braking. Thereafter, it is necessary to suppose a strong Skumanich braking law (i.e a large value of K_{sk}) to fit the braking at later ages down the solar value. But a main problem remains for initial ultra fast rotators as they cannot spin-down enough to reach convergence at the age of the Sun. Furthermore, with this model, a strong differential rotation remains inside the star at the age of the Sun: for the slowest rotators, the radiative core still rotates 4 times as fast than the envelope, and for fastest rotators, the core rotates 10 times as fast. And this is in contradiction with the observations of the angular velocities in the solar interior.

Another problem arises with Alpha Per's rapid rotators, as the maximum velocity achieved is only 100 km s^{-1} . A larger initial velocity would lead to a larger velocity at ZAMS ages. But such rapid rotators would also lead to far too large velocities during MS phase (see Fig. 12).

Model of 0.8 and $0.6 M_{\odot}$ require, respectively, $\Omega_{sat} = 5$ and $4 \Omega_{\odot}$ (Fig 13 and 14). In young clusters, the same holds for 0.8 and $0.6 M_{\odot}$ models as for the $1 M_{\odot}$ model: it is difficult to fit rapid rotators, but the fits of slow rotators are quite good. Conversely, for the Hyades cluster, 0.6 and $0.8 M_{\odot}$ models lead to a spread larger than observed, while the $1 M_{\odot}$ model spread fits the data well.

For $0.5 M_{\odot}$, Ω_{sat} is set to $1.2 \Omega_{\odot}$ to account for ZAMS rapid rotators. Evolutionary tracks look quite the same as in other coupling time models for the same mass to the age of the Pleiades. The differences to other coupling time models occur after the ZAMS, where braking is much more rapid. Therefore, at the age of the Hyades, this model cannot account for the fastest rotators ($50 \Omega_{\odot}$). It also finds a lower limit ($1 \Omega_{\odot}$) which is too low, whereas Hyades slow rotators have rotation rate between 4 and $8 \Omega_{\odot}$. The long coupling-time is still too long compared to the evolutionary time, and as for the 0.8 or $0.6 M_{\odot}$ models in M 34, it leads to too slow rotators during the MS phase. This model would eventually require a weaker braking law to reproduce the $0.5 M_{\odot}$ Hyades members.

The main successes of this model is to easily explain 1) the rapid decrease of rapid rotators between Alpha Per and the Pleiades, and 2) the existence of a large number of very slow rotators from T Tauri ages to the age of the Sun in the $0.9\text{--}1.1 M_{\odot}$ mass range without requiring long disk lifetimes. But this model cannot reproduce 1) ZAMS rapid rotators, 2) braking of rapid rotators during the main sequence, 3) large velocities of low-mass stars in the Hyades cluster and 3) the rotational profile of the Sun.

6. Discussion and conclusions

The main assumption of the model presented here is a decoupling between the stellar core and the envelope, and the existence of angular momentum transfer, controlled by a coupling time-scale τ_c . I computed evolutionary tracks for 3 different coupling time-scales and compared the results to the observations. If the coupling time-scale is short compared to the contraction time scale (a few Myr vs a few 10 Myr), then the star will nearly rotate as a solid-body. If it is long, then decoupling will have

non negligible effects on rotational evolution. I first summarize the effects of the models presented here.

With a long coupling time model (i.e. 500 Myr) it is very easy to keep a low surface velocity, as wind braking only applies on the envelope. This model leads to quite a good agreement with the slow rotators fraction at ZAMS ages, even if only short disk lifetimes are considered (≤ 10 Myr). Rapid braking of rapid rotators between the age of Alpha Per and the Pleiades is also in good agreement with the observations. However, it is more difficult to explain the existence of these rapid rotators on the ZAMS. The existence of rapid rotators requires a weak braking law, inconsistent with the subsequent rapid braking. Furthermore due to the angular momentum core resurfacing, braking nearly stops on the MS, in contradiction with the observations. With a coupling time of 500 Myr, the angular momentum transfer from the core to the envelope really becomes effective at the age of the M 34/M 7 clusters, and is far from being finished by the age of the Sun. The internal rotational profile of the Sun thus cannot be reproduced.

Results for an intermediate coupling time (20 Myr) are worse for both rapid and slow rotators. In young clusters such as Alpha Per and the Pleiades, the problem is the same as in the long coupling time model: rapid rotators require a weak braking law to arise, but rapid spin-down requires a strong braking law. As the coupling time is in the order of the age of these clusters, angular momentum transfer begins to be effective. This leads to an increase of the velocities of very slow rotators, and braking of rapid rotators occurs only on a very short time scale. In older clusters such as M 34 and the Hyades, the transfer is in progress, so that braking is slow, and the model predicts too large velocities. At the age of the Sun, however, the transfer is finished and the star is a quasi-solid body, even for the most rapid rotators.

The main problem of the short coupling time model (1 Myr) is the existence of a large number of slow rotators in young clusters. The only process that keeps the star from spinning up is the disk-locking. It is then necessary to suppose that a fraction of the disks can survive as long as 40 Myr. A short coupling time can easily reproduce rapid rotators on the ZAMS and rapid decrease of these rotators from the age of Alpha Per for $1 M_{\odot}$ stars (and from the age of the Pleiades for lower masses) to the age of the Sun. This model is also in good agreement with the observed solar rotational profile.

As pointed out in Sect. 3.2, most of the theories of angular momentum transfer predict that the coupling time is a function of angular velocity (core, envelope or both). In a way, the effect of the difference between the core and envelope rotational velocities is taken into account in the angular momentum exchanges quantity ΔJ . In spite of this, rapid rotators are easier to account for with solid-body rotation, over the all mass range, while slow rotators are well fitted with a strongly decoupled model. For the latter, the coupling time scale should be at least of order of the age of the Pleiades (100 Myr) so that angular momentum transfer is only effective on the main sequence, thus allowing ZAMS slow rotators. On the other hand, the coupling time scale should not be much longer so that there is no important differential rotation left at the age of the Sun.

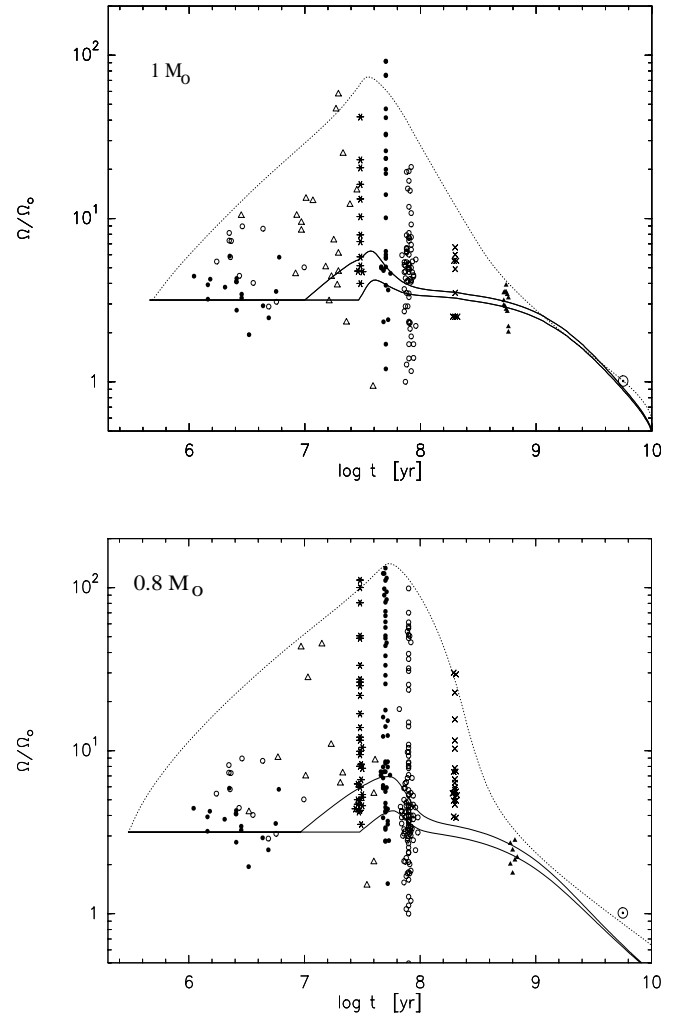


Fig. 16. Evolutionary tracks for $1 M_{\odot}$ (upper panel) and $0.8 M_{\odot}$ (lower panel) and an initial period of 8 days. Dotted line represents a solid-body rotation model ($\tau_c = 10^6$ yr), solid line represents a decoupled model ($\tau_c = 10^8$ yr). Tracks are represented for 3 different disk-lifetimes: 0.5, 10 and 30 Myr for $1 M_{\odot}$ and 0.3, 10 and 30 Myr for $0.8 M_{\odot}$.

Fig. 16 presents the evolutionary tracks for 0.8 and $1 M_{\odot}$ models with an initial period of 8 days, and with two different coupling times: I use a short coupling time to fit rapid rotators, and a model with a coupling time of 100 Myr to fit slow rotators. As discussed in previous section and in this one, a solid-body model is able to reproduce the braking of rapid rotators all over the main sequence phase for both masses. On the other hand, the model with $\tau_c = 100$ Myr can easily explain existence of slow rotators in the $0.9\text{--}1.1 M_{\odot}$ mass range with disk-lifetimes of 10 Myr at most. The tracks presented in Fig. 16 start with an initial period of 8 days and can fit velocities as low as 6 km s^{-1} at the age of the Pleiades, i.e an important fraction of the stars in the Pleiades. A T Tauri distribution with periods up to 16 days can explain the existence of the Pleiades very slow rotators which have velocities lower than 6 km s^{-1} .

But ZAMS slow rotators still pose severe problems to the models. Slow rotators in the mass range $0.6\text{--}0.9 M_{\odot}$ are more difficult to account for because they are more numerous, and also because a $0.8 M_{\odot}$ model leads to a higher velocity at the Pleiades age, than a $1 M_{\odot}$ model (using the same initial period and disk lifetime).

In their paper, Krishnamurthi et al. (1997) claimed that there is a significant decrease of the fraction of slow rotators between the age of Alpha Per and the age of the Pleiades: there are no stars in the velocity range $0\text{--}7.5 \text{ km s}^{-1}$ in Alpha Per, while 10% of the Pleiades stars have velocities lower than 7.5 km s^{-1} . But recent *vsini* observations in these clusters – presented on the figures of rotational evolution – show that 1) stars in the mass range $0.9\text{--}1.1 M_{\odot}$ with velocities lower than 6 km s^{-1} are not braked, 2) stars with *vsini* lower than 10 km s^{-1} are only slightly braked, 3) stars in the mass range $0.6\text{--}0.9 M_{\odot}$ are significantly braked at all velocities (Queloz et al. 1997a, 1997b, Allain et al. 1997).

It seems to be different at early ages. The mean rotation in the young clusters IC2391 and IC2602 (30 Myr) is higher than in Alpha Per. But for older clusters, there is no evidence that the mean rotation in M 34 is larger than in the Pleiades. Conversely, Hyades' mean rotation is definitely lower than in the Pleiades.

How slow rotators evolve during the ZAMS and early-MS phases is a crucial issue to constrain the models. From Fig. 16, results for $\tau_c = 100$ Myr are in good agreement with the $1 M_{\odot}$ observations of very slow rotators but this model seems predicts a too important braking for rotators with velocities between 10 and 20 km s^{-1} . On the other hand, this model finds a braking for slow rotators in the mass range $0.6\text{--}0.9 M_{\odot}$ consistent with the observations, while a solid-body model cannot brake these stars.

From the results presented on this paper, I conclude that rapid rotators can be assimilated to solid bodies, and that slow rotators are submitted to an important differential rotation. The parametric description used here is however too basic to explain velocity effects, especially for moderate rotators, and a more physical description, handling angular momentum transfer in the radiative core, is required. Masses effects – probably through the depth of the convective zone – are also very important in angular momentum transfer. More observations are clearly needed to constrain the models both at different ages and different masses.

Acknowledgements. I wish to thank J. Matias, J.-P. Zahn and S. Talon for interesting discussions, M. Forestini for providing evolutionary codes, and J. Bouvier for helpful comments

References

- Allain S., Bouvier J., Prosser C.F., Marschall L.A., Laaksonen B.D., 1996a, A&A 305, 498
- Allain S., Mayor M., Queloz D., Fernández M., Martín E.L., Bouvier J., Mermilliod J.C. 1996b, in 9th Cambridge Workshop on Cool Stars, Stellar System and the Sun, eds R. Pallavicini & A.K. Dupree, in press
- Allain S., Queloz D., Bouvier J., Mermilliod J.C., Mayor M., 1997 in “Cool stars in clusters: magnetic activity and age indicator” in press
- Armitage P.J., Clarke C.J. 1996, MNRAS 280, 458
- Basri G., 1997 in “Cool stars in clusters: magnetic activity and age indicator” in press
- Bouvier J., Bertout C., Benz W., Mayor M., 1986, A&A 165, 110
- Bouvier J., AJ 99, 646
- Bouvier J. 1991, in Angular Momentum Evolution of Young Stars. S. Catalano & J.R. Stauffer, eds, Kluwer Academic Publishers, Dordrecht, NATO ASI Series
- Bouvier J., Cabrit S., Fernández M., Martín E.L., Matthews J. 1993, A&A 272, 167
- Bouvier J, Forestini M. 1995, in “Circumstellar dust disk and planetary formation”, 10th IAP meeting, eds Ferlet, p. 347
- Bouvier J. Covino E., Kovo O., Martin E.L., Matthews J.M., Terranegra L., Beck S.C. 1995, A&A 299, 89
- Bouvier J., Wichmann R., Grankin K., Allain S., Covino E., Fernandez M., Martin E.L., Terranegra L., Catalano S., Marilli E., 1997a, A&A in press
- Bouvier J., Forestini M., Allain S., 1997b, A&A submitted
- Cameron A.C., Campbell C.G. 1993, A&A 274, 309
- Cameron A.C., Campbell C.G., Quaintrell H., 1995, A&A 298 133
- Cameron A.C., Li Jianke, 1994, MNRAS 269, 1099
- Chaboyer B., Demarque P. and Pinsonneault M.H., 1993, ApJ 441, 865
- Charbonneau P., 1992, in 7th Cambridge Workshop on Cool Stars, Stellar System and the Sun, ASP. Conf Series, Vol. 26, eds Giampapa & Bookbinder, p.416
- Charbonneau P., McGregor K.B., 1993, ApJ 417, 762
- Covino E. et al. 1997 submitted
- Endel A.S., Sofia S., 1978, ApJ 220, 279
- Eddington A.S., 1925, Observatory, 48, 73
- Edwards S. et al. 1993, AJ 106, 372
- Forestini M., 1994, A&A 285, 473
- Fricke K., 1968, Z. Astrophys., 68, 317
- Goldreich P., Schubert G., 1967, ApJ, 150, 571
- Gough D.O., 1991, in Angular Momentum Evolution of Young Stars. S. Catalano & J.R. Stauffer, eds, Kluwer Academic Publishers, Dordrecht, NATO ASI Series
- Jones B.F, Fischer D., Shetrone M., Soderblom D.R., 1997, in press
- Kawaler S.D., 1988, ApJ 333, 236
- Keppens R., MacGregor K.B, Charbonneau P., 1995, A&A 294, 469
- King A.R. & Regev O. 1994, MNRAS 268, L69
- Königl A. 1991, ApJ 37, L39
- Krishnamurthi A., Pinsonneault M.H., Barnes S., Sofia S., 1997, ApJ 480, in press
- Kumar P., Quataert E.J. 1997, ApJ 475, 143
- Endel A.S., Sofia S., 1978, ApJ 220, 279
- Li Jianke & Collier Cameron A., 1993, MNRAS 261, 766
- Matias J., Zahn J.-P., 1997, A&A
- Mayor M., Mermilliod J.-C. 1991, in “Angular momentum evolution of young stars”, eds S. Catalano and J.R. Stauffer, p.117
- McGregor K.B., Brenner M., 1991, ApJ 376, 204
- McGregor K.B., 1991, in “Angular momentum evolution of young stars”, eds S. Catalano and J.R. Stauffer, p.315
- Mestel, L., Taylor, R.L., Moss, D.L. 1988, MNRAS 231, 873
- Press W.H., 1981, ApJ, 245, 286
- Prosser C.F. 1992, AJ 103, 488
- Prosser C.F. 1992, AJ 107, 422
- Prosser C.F., Stauffer J.R., Caillault J.-P., Balachandran S., Stern R.A., Randich S. 1995 AJ, 110, 1229

- Queloz D., Allain S., Mermilliod J.C., Bouvier J., Mayor M., 1997a
A&A in press
- Queloz D., Allain S., Mermilliod J.C., Bouvier J., Mayor M., 1997b
in "Cool stars in clusters: magnetic activity and age indicator" in
press
- Radick R.R., Thompson D.T., Lockwood G.W., Duncan D.K., Bagget
W.E 1987 ApJ 321, 459
- Schatzman E., 1962, Ann Astr 25, 1
- Schatzman E., 1993, A&A 279, 431
- Shu F., Najita J., Ostriker E., Wilkin F., Ruden S., Lizano S. 1994, ApJ
429, 781
- Skumanich A. 1972, ApJ 171, 565
- Soderblom D.R., Stauffer J.R., Hudon J.D., Jones B.F., 1993, ApJS 85,
315
- Stauffer J.R., Balachandran S., Krishnamurthi A., Pinsonneault M.H.,
Terndrup D.M., Stern R.A., 1997a, ApJ, 475, 87
- Stauffer J.R., Hartmann L.W., Prosser C.F., Randich S., Balachandran
S., Patten B.M., Simon T., Giampapa M., 1997b, ApJ, 479, 776
- Stauffer et al. 1997c, private communication
- Talon S., Zahn J.-P., Maeder A., Meynet G. 1997, A&A, in press
- Tassoul M., Tassoul J.-L., 1995, ApJ, 440, 789
- Tomczyk S., Schou J., Thompson M.J., 1996, BAAS, 188, 69.03
- Weber E.J., Davis L. 1967, ApJ 148, 217
- Zahn J.-P. 1992, A&A 265, 115
- Zahn J.-P., 1996 SCORE, Aarhus, ed. F. Rippers
- Zahn J.-P., Talon S., Matias J, 1997, A&A, in press
- Wichmann R., Bouvier J., Allain S., Krautter J., 1997, A&A submitted